

Energy and transition-rate dependent neutralisation of secondary ions originating from inner-shell excitation

Klaus Wittmaack*

The observation of comparatively high yields of low-energy secondary ions (emission energy < 100 eV), ejected from clean ion bombarded solids, has been a long standing miracle. At the corresponding low velocities, the observed velocity dependence of the ionization probability is in variance with the predictions of the resonant-tunnelling model. It has been proposed that the measured high yields are due to electronic excitations initiated by the collision cascade, the consequence being a significantly altered electron density distribution at the solid surface. Here the issue is addressed by exploring energy spectra of ions generated by inner shell electron promotion. Using new experimental results and literature data, ionisation probabilities were determined using two different approaches. Above element-specific critical emission velocities v_{crit} the results are largely in accordance with the resonant-tunnelling model which predicts an exponential velocity dependence of the neutralisation probability P . For $v < v_{\text{crit}}$, however, P approaches a constant level, largely independent of the velocity v and much higher than predicted by the tunnelling model. The results imply that, under certain circumstances and in a relatively small fraction of ejection events, neutralisation of ions formed in the immediate vicinity of the surface is blocked. Given the fact that we are dealing with ionisation energies > 18 eV, the electronic-excitation model can hardly explain these observations. It is suggested that neutralization may be blocked if the collision cascade causes a very high perturbation of the surface, to the end that the departing will interact only with a dense cloud of atoms but not with a solid featuring a well-defined band structure (on which some electronic excitation may be superimposed). Even though these events are rare, the effect is large because, in the absence of perturbation, the ion yields would be very low.

Keywords: secondary ion mass spectrometry, SIMS, inner-shell excitation, neutralisation

* Correspondence to: Klaus Wittmaack, Helmholtz Zentrum München, Institute of Radiation Protection, 85758 Neuherberg, Germany
Email: wittmaack@gsf.de

Introduction

Even after several decades of research, the basic mechanisms leading to secondary ion formation in sputtering of solid samples are not known in any detail. A reasonable level of understanding has only been achieved in comparatively simple situations, e.g. when tailoring the experiment to strongly enhance negative secondary ion yields by depositing sub-monolayer quantities of alkali metals on the analysed surface. In that case the ion fraction observed far away from the surface, commonly referred to as the ionization probability P^- , can be described in terms of the resonant-tunnelling model,^{1,2,3}

$$P^- = A \exp(-v_0/v), \quad (1)$$

where v is the velocity of the departing atom/ion normal to the sample surface, v_0 is a parameter describing the width of the affinity level, and A an element specific constant close to, but less than unity. Applying this model to positive secondary ion emission from clean metal surfaces, reasonable agreement with Eq. (1) has been observed at comparatively high velocities. At low velocities, however, the measured ionization probabilities were much higher than expected on the basis of the assumed exponential $1/v$ dependence.^{2,3,4,5} It has also been argued^{6,7} that for ionization probabilities $P^+ < 10^{-4}$, often observed in positive secondary ion emission from clean solids,⁸ the applicability of Eq. (1) would imply that, in contrast to experimental findings, the peaks in the secondary ion energy spectra should be located well above 50 eV. Last, but not least, positive secondary ion yields were observed to increase with increasing primary ion energy,^{9,10} an effect not contained in Eq. (1).

To account for deviations from Eq. (1), Šroubek et al.¹¹ introduced the idea that, apart from generating a collision cascade that leads to sputtering, the impact of energetic ions will also produce sizable electronic excitations which may tentatively be described by a local electron temperature,¹² quite high and sufficiently long-lasting to cause significant ionisation of low-energy sputtered atoms. The concept has been extended recently using molecular dynamics simulations,¹³ but quantitative predictions of ion yields are not yet available. Objections against a quasi-thermodynamic description of ion formation have been raised on the basis of the argument that the conceivable “increase of the electronic temperature is very small due to both weak electron-electron interactions and (an) insufficient quantity of conduction electrons participating in this process”.¹⁴

A completely different approach towards explaining the cited results is to assume that, locally and for a short period of time, the bulk electronic properties of the sample are destroyed by ion bombardment.⁸ This kind of extreme “dynamic randomisation” could significantly lower the neutralisation probability. Evidence for dynamic randomisation has been found in the angular distributions of atoms sputtered from samples of single crystalline gold.^{15,16} The importance of a strongly altered local electronic structure has been investigated theoretically,¹⁷ but, unfortunately, the idea was not pursued any further.

The aim of this study was to explore secondary ion emission under conditions such that communication of the (excited) atom with the solid can hardly be affected by excitations of the electronic system of the target. Owing to the high energy required for producing doubly charged secondary ions (typically > 18 eV),

they are ideally suited for the purpose in question. The formation of these ions involves three steps, (1) inner shell excitation by electron promotion,¹⁸ (2) transport of the ions with an inner-shell hole from the solid into vacuum and (3) Auger deexcitation to form doubly charged ions. Singly charged ions may also be formed this way. Details of inner shell excitation at primary ion energies ≤ 15 keV have been studied mostly by Auger electron spectroscopy,¹⁹ but it was confirmed that the yields of atomic-like Auger electron signals originating from sputtered atoms and the yields of doubly charged secondary ions are intimately correlated.²⁰

Experiment

The ultrahigh-vacuum, quadrupole based SIMS instrument used in this study has been described elsewhere.²¹ It allows secondary ion energy spectra to be recorded with a resolution of 2 eV or better. Ions with energy-to-charge ratios $E/q < 100$ V could be analysed without sizable changes in instrument transmission. Clean Si and Ti targets were bombarded with either 10 or 12 keV Ar^+ ions at 2° off normal.

To extend the available experimental data to secondary ion energies not accessible in standard quadrupole based instruments, results previously obtained by Schauer and Williams²² using a magnetic sector field instrument, a Cameca IMS-3f, were included in the evaluation. Doubly charged secondary ion emission from third and fourth-row elements was investigated under impact of Ar^+ ions at an energy of 8 keV (\pm the energy change due to the scanning the target bias). After modifying the equipment, energy spectra could be recorded up to $E/q = 500$ V. To improve sensitivity, but at the expense of an accurate definition of the origin of the energy scale, the band pass of the electrostatic sector field analyser was set to 20 qV. In the evaluation presented below it was assumed that the frequently observed low-energy peak due to gas phase ionisation²³ defines the origin of the energy scale, $E = 0$. The resulting modifications to the original energy scale varied somewhat between target materials, from about +12 eV to -15 V.

Data evaluation

Analysis of the energy spectra recorded in this study was based on a modified version of Eq. (1). Let $N^*(E)$ denote the energy spectrum of ejected excited ions. Setting $A = 1$ in Eq. (1), scaled secondary ion energy spectra $y(E)$ of clean samples were derived from measured spectra $I(E)$ as

$$y(E) = bI(E) = N^*(E)P(v) = N^*(E) \exp(-v_0/v), \quad (2)$$

The scaling factor b contains parameters like the instrument transmission and the excitation probability. $N^*(E)$ was set equal to the Thompson distribution²⁴ of sputtered neutrals, $N^0(E)$, with $\int N^0(E)dE = 1$ (surface binding energies $E_s(\text{Si}) = 4.7$ eV and $E_s(\text{Ti}) = 4.9$ eV).

As to the results of Schauer and Williams, experimental data were extracted from the original publication²² at suitable energy intervals. M^{2+} energy spectra were reported for clean samples analysed in high vacuum as well as for samples exposed to an oxygen jet. The latter spectra provided an alternative route for data evaluation without an assumption concerning $N^*(E)$. The idea was that under conditions of (the assumed) full oxidation the lack of conduction electrons results in a strongly reduced or even completely

suppressed neutralization. Hence, the energy spectra of oxidized samples, $I^{\text{ox}}(E)$, were assumed to represent $N^*(E)$ so that

$$P(E) = I(E)/kI^{\text{ox}}(E). \quad (3)$$

The fitting factor k accounts for differences in sputtering yield due to sample oxidation^{25,26} as well as for possible differences in the cross section for inner-shell excitation. For ease of discussion k was chosen so that $P(v) \rightarrow 1$ for $E \rightarrow \infty$, i.e. for $1/v \rightarrow 0$. Note that by way of taking ratios the energy dependent transmission of the instrument⁷ cancels out.

Results and Discussion

Quadrupole based data

Experimentally determined energy spectra of $^{30}\text{Si}^{2+}$ are presented in Fig. 1 as open circles and solid triangles. Data evaluation according to Eq. (2) showed that a good fit to the measured Si^{2+} spectrum in the range $10 < E < 120$ eV can only be achieved within a rather narrow range of the parameters v_0 and b . The derived low value $v_0 = 0.11 \pm 0.01$ Å/fs implies that the ionisation probabilities were quite high, 26% at 10 eV and 65% at 100 eV ($v = 0.082$ and 0.258 Å/fs, respectively). The emission of Si^{2+} ions involves the formation of 2p holes for which the $L_{2,3}$ Auger transition rate ν_{2p} has been calculated^{27,28} as $\nu_{2p}(\text{Si}) = 2.3 \pm 0.4 \times 10^{13} \text{ s}^{-1}$ (corresponding lifetime $\tau_{2p} = 44 \pm 9$ fs). The product $v_0 \tau_{2p} \equiv z_0 = 4.8 \pm 1.0$ Å defines a characteristic distance of neutralization. This number is only a factor of about two larger than the distance of maximum electron exchange activity in the tunnelling model.³ The reasonable value of z_0 supports the assertion that, under the chosen operating conditions of the energy filter and the quadrupole, the instrument transmission was fairly independent of energy.

Turning to the results for Ti^{2+} in Fig. 2 we first note that, according to ion induced Auger spectra observed at impact energies between 5 to 15 keV,^{29,30} the production of Ti^{2+} ions must be attributed to $M_{2,3}$ inner shell excitation. The large difference between the Ti^{2+} spectrum in Fig. 2 and the Si^{2+} spectrum in Fig. 1 is evident at first sight. A maximum in the measured Ti^{2+} energy spectrum is not observed up to 230 eV. The fitted spectrum $y(E)$ suggests that a maximum might exist between about 300 and 400 eV. Below 100 eV the experimentally derived Ti^{2+} ion fractions are much larger than predicted by Eq. 2. The deviations increase with decreasing energy. The strongly reduced yield of Ti^{2+} ions implies a large characteristic velocity v_0 . The fitting procedure yielded $v_0 = 1.3$ Å/fs, a number that is larger by a factor of 12 than for Si^{2+} . The difference can be attributed to a rather short lifetimes of holes in the $M_{2(3)}$ -shell, calculated³¹ to be 3.1 fs. The resulting z_0 -value is 4.0 Å, close to the result for Si^{2+} .

Also shown in Fig. 2 are results for Ar^+ reemitted under stationary Ar bombardment of Ti. Production of $L_{2,3}$ holes in is mostly due to asymmetrical collision Ar-Ti collisions,³² but the probability for hole production is low, as one can tell from the rather low b -values required for fitting. In terms of the expected position of the maximum, the spectra due to Ar^+ and Ti^{2+} are quite similar. Hence v_0 -value derived for Ar^+

(1.5 Å/fs) is almost the same as for Ti^{2+} . With a calculated lifetime^{27,28} of 4.5 fs we have $z_0 = 6.7$ Å. The small but distinct differences in the evaluated characteristic velocities for Ti^{2+} and Ar^+ may be responsible for the observed differences in the shape of the scaled spectra at energies below 100 eV.

To summarize this first part of the results and the data evaluation, the analysis suggests that measured energy spectra of secondary ions originating from inner-shell excitation comply with an exponential velocity dependence of the neutralisation probability, but only beyond some critical energy or velocity v_{crit} of emission, with is loosely related to the characteristic velocity v_0 describing neutralization at high velocities ($v_{\text{crit}} = 0.2 \dots 0.6 v_0$). At emission velocities below v_0 the measured ion yields exceed the predicted values, more so the lower the emission energy or velocity. This deviation calls for an explanation.

Analysis of magnetic sector-field data

Normalized ionization probabilities derived on the basis of Eq. (3) from the energy spectra reported by Schauer and Williams are presented in Fig. 3 as a function of emission energy. Also shown are ionisation probabilities according to the resonant-tunnelling model (dash-dotted lines). The data for Mg, Al and Si reflect the fact that the transition rates for these elements are rather low ($< 2.3 \times 10^{13} \text{ s}^{-1}$) so that one expects little neutralisation even in the case of emission from clean targets (normalized ionisation probability $\cong 1$). These data also provide an estimate for the level of uncertainty involved in the evaluation. The message of Fig. 3 is the same as of Figs. 1 and 2: At high energies the ionisation probabilities derived from experimental data are in accordance with the predictions of the resonant-tunnelling model. At low energies, however, the ‘measured’ ion yields are much higher than predicted.

In Fig. 4, the data for the fourth-row elements are also shown versus the inverse velocity $1/v$. At low values of $1/v$, i.e. at high velocities, the ion fractions are in reasonable accordance with a dependence of the form $\exp(-v_0/v)$. The v_0 -values producing the best fit to the high-velocity data increase with increasing atomic number of the element under study, rapidly first (Ca \rightarrow Sc), but then more slowly. This is exactly the same trend as for the transition rates in Fig. 3.

The close correlation between v_0 and the $M_{2,3}$ transition rate is documented in Fig. 5. Note that the v_0 -values derived for Ti from experimental data measured with two completely different instruments and evaluated in two ways agree very well. This excellent agreement raises the question to what extent the choice of the reference spectrum $N^*(E)$ in Eq. (2) will affect the differences between experimental data and theoretical predictions. This question has been explored by using Thompson distributions instead of the spectra of oxidized samples for reference purposes. Appropriate high-energy cut-offs in accordance with TRIM.SP simulations³³ were superimposed on the assumed energy distribution of neutrals. Depending on the element, the v_0 -values thus derived were typically a factor of two higher than by using the spectra of the oxidized samples as a reference. But the general trend remained the same, i.e. below some critical velocity

the ionization probabilities derived from experimental data were higher than predicted, more so the lower the energy.

One additional aspect is worth mentioning. The crosses and the dashed line in Fig. 5 represent the deviation of the ‘experimental’ data from the theoretical predictions. The data suggest that the additional contribution to the theoretical values is largely independent of the ion velocity.

Considering the fact that in this study we have specifically addressed the emission of secondary ions originating from inner-shell excitation, the observation of a largely velocity independent contribution cannot be explained in terms of a quasi-thermal excitation model. If we retain the idea that neutralization is controlled by the transfer of conduction electrons from the target to the departing ion, the only reasonable explanation for the observed results is that, in a sizable fraction of impact and emission events, neutralization must be blocked (almost) completely. In these events the target surface left behind by the departing ions must have been highly perturbed, with no significant short-range order left, so that a band structure is no longer defined for a period of time on the order of femtoseconds *after ejection*. Hence the ion can only interact with other atoms and ions, not with the electronic system of a solid, thus avoiding neutralization. This model of suppressed neutralization can be applied to singly-charged ion emission as well. In fact, a recent analysis³ of the fraction of In^+ in the total sputtered flux, measured by laser post ionization,⁵ revealed the same picture as the data in Fig. 5, only shifted to much lower energies.

Energy spectra of excited neutrals

Ideally one would like to know the energy spectrum of excited neutrals. Some of the expected trends have been discussed by Sigmund,³⁴ by analytical expression are not yet available. If the assumption on which the evaluation of the data in Figs. 3 and 4 is based is correct, the energy spectra of doubly charged secondary ions emitted from oxidized metals would reflect the spectrum of excited neutrals, but multiplied by the transmission function of the spectrometer. To first order the transmission can be expected to scale as $1/E$. Normalised energy spectra of excited neutrals, derived from measured energy spectra of doubly charged ions²² after correction for transmission, are compiled in Fig. 6. Somewhat surprisingly, the spectra of the third-row and the fourth-row elements exhibit distinct if not large differences. Whereas the spectra for the fourth-row elements are almost flat over a wide range of ejection energies, i.e. from about 40 to 300 eV, the spectra of Si and Al exhibit well defined peaks around 30 eV (less pronounced for Mg). The origin of this difference is not clear. Note that the low-energy peak is most pronounced for the element featuring the highest inner shell excitation energy (Si). This finding may provide some justification for using a Thompson-type distribution for fitting the data of Fig. 1. On the other hand it is clear that much more work will be required in order to understand the extracted spectral features shown in Fig. 6.

Conclusion

The results of this study suggest that the observed high yields of low-energy secondary ions originating from sputtered atoms with an inner shell hole are due to suppressed neutralization. It is argued that for some period

of time during a sputtering event, the surface may be so highly perturbed around the point of emission that a solid-state conduction band does not exist locally, i.e. there is no supply of the electron(s) that are required for neutralization. The measured ion fractions reflect the (low) probability for this to happen. In the absence of heavy perturbations, the yields of secondary ions with energies < 50 eV would be expected to be much lower, i.e. at or below the detection limit of standard instruments (except for elements with $v_0 \leq 0.2$ Å/fs). It would be interesting to study the sketched scenario of surface perturbations during sputtering by extracting the required information from the molecular dynamics simulations currently performed by many groups in the field of ion-solid interactions.

Fig. 1. Normalized energy spectra of doubly charged Si secondary ions sputtered from clean silicon. Symbols: experimental data; dashed and dash-dotted lines: spectra fitted according to Eq. (2).

Fig. 2. The same as Fig. 1, but for the emission of doubly charged Ti and singly charged Ar ions emitted from argon bombarded clean titanium.

Fig.3. Normalized ionisation probabilities of doubly charged secondary ions for clean elemental targets of the third and fourth row of the periodic table, derived from energy spectra of clean and oxidized targets (raw data of Schauer and Williams, ref. 22).

Fig. 4. The same as Fig. 3, but as a function of the inverse velocity of the emitted ions (fourth-row elements only). The crosses and the dashed line denote the difference between the evaluated data and the assumed exponential $1/v$ -dependence of the ionization probability for Ti.

FIG. 5. Characteristic velocities v_0 versus calculated transition rates (refs. 27, 28, 31). The $M_{2,3}$ transition rate for Sc was derived by interpolation. The lines are guides to the eye.

Fig. 6. Energy spectra of doubly charged secondary ions emitted from oxidized targets, corrected for energy dependent instrument transmission. The spectra are normalised to unit integral. Raw data from ref. 22.

References

- [1] M. L. Yu, N. D. Lang, *Phys. Rev. Lett.* **1983**, 50, 127.
- [2] Z. Šroubek, J. Lörinčík, *Surf. Rev. Lett.* **1999**, 6, 257.
- [3] K. Wittmaack, *Mat. Fys. Medd. Dan. Vid. Selsk.* **2006**, 52, 465.
- [4] A. Wucher, H. Oechsner, *Surf. Sci.* **1988**, 199, 567.
- [5] P. Mazarov, A. V. Samartsev, A. Wucher, *Appl. Surf. Sci.* **2006**, 252, 6452.
- [6] K. Wittmaack, *Physica Scripta* **1983**, T6, 71.
- [7] K. Wittmaack, *Surf. Sci.* **1999**, 429, 84.
- [8] R. G. Wilson, S. W. Novak, *J. Appl. Phys.* **1991**, 69, 466.
- [9] K. Wittmaack, *Surf. Sci.* **1979**, 90, 557.
- [10] Z. Šroubek, *Appl. Phys. Lett.* **1983**, 42, 514.
- [11] Z. Šroubek, K. Ždánsky, J. Zavadil, *Phys. Rev Lett.* **1980**, 45, 580.
- [12] Z. Šroubek, J. Lörinčík, *Vacuum* **2000**, 56, 263.
- [13] A. Duvenbeck, A. Wucher, *Phys. Rev. B* **2005**, 72, 165408.
- [14] V. I. Veksler, *Vacuum* **2004**, 72, 277.
- [15] R. S. Nelson, *Rad. Effects* **1971**, 7, 263.
- [16] W. Szymczak, K. Wittmaack, *Nucl. Instrum. Methods Phys. Res. B* **1993**, 82, 220.
- [17] A. Nourtier, J.-P. Jardin, J. Quazza, *Phys. Rev.* **1988**, 37, 10628.
- [18] U. Fano, W. Lichten, *Phys. Rev. Lett.* **1965**, 14, 627.
- [19] S. Valeri, *Surf. Sci. Rep.* **1993**, 17, 85.
- [20] K. Wittmaack, *Nucl. Instrum. Methods* **1980**, 170, 565.
- [21] K. Wittmaack, *Surf. Sci.* **1996**, 345, 110.
- [22] S. N. Schauer, P. Williams, *Phys. Rev. B* **1992**, 46, 15452.
- [23] K. Wittmaack, *Int. J. Mass Spectrom.* **2008**, 269, 24.
- [24] M. W. Thompson, *Phil. Mag.* **1968**, 18, 377.
- [25] A. E. Morgan, H. A. M. de Grefte, N. Warmoltz, H. W. Werner, *Appl. Surf. Sci.* **1981**, 7, 372.
- [26] K. Wittmaack, S. F. Corcoran, *J. Vac. Sci. Technol. B* **1998**, 16, 272.
- [27] E. J. McGuire, *Phys. Rev. A* **1971**, 3, 587.
- [28] D. L. Walters and C. P. Bhalla, *Phys. Rev. A* **1971**, 4, 2164.
- [29] P. Viaris de Lesegno, J.-F. Hennequin, *J. Physique* **1974**, 35, 759.
- [30] K. F. Kam, T. E. Gallon, J. A. D. Matthew, C. Kersten, *J. Phys.: Condens. Matter* **1999**, 11, 5723.
- [31] E. J. McGuire, *Phys. Rev. A* **1972**, 5, 1052.
- [32] Viaris de Lesegno and J.-F. Hennequin, *Surf. Sci.* **1979**, 80, 656.
- [33] W. Eckstein and J. P. Biersack, *Z. Phys. B – Cond. Mat.* **1986**, 63, 109.
- [34] P. Sigmund, in *Inelastic Particle-Surface Collisions*, edited by E. Taglauer and W. Heiland (Springer, Berlin, 1981) p. 251.

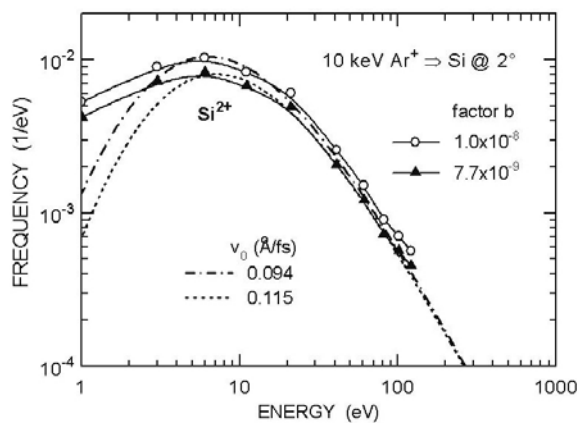


Fig. 1

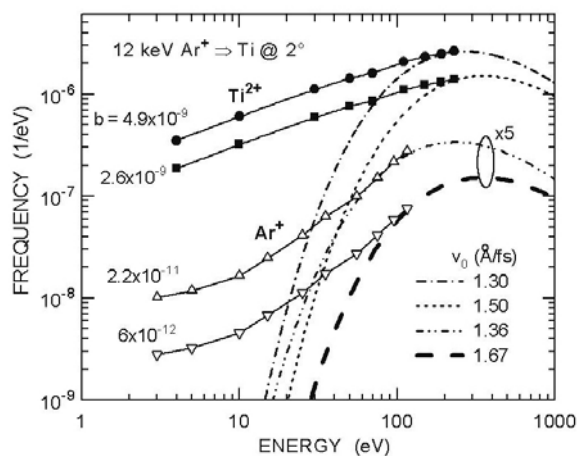


Fig. 2

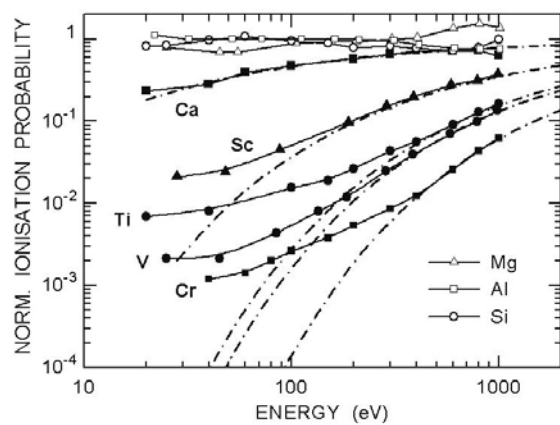


Fig. 3

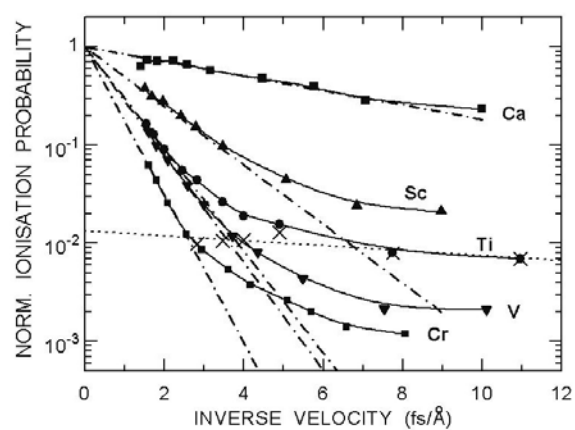


Fig. 4

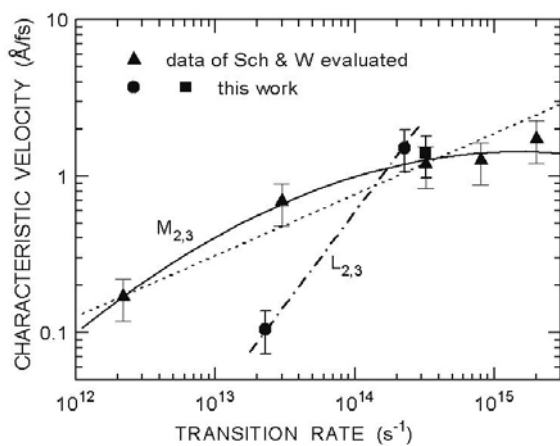


Fig. 5

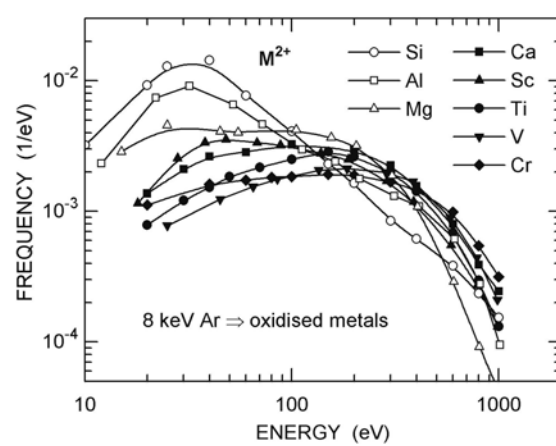


Fig. 6